

# Effect of A Moving Obstacle on Pedestrian Evacuation Simulation Using Social Force Model

Han Xu · Weiguo Song · Jun Zhang

State Key Laboratory of Fire Science, University of Science and Technology of China, Hefei, China,  
E-mail: [pgdabb@mail.ustc.edu.cn](mailto:pgdabb@mail.ustc.edu.cn), [wgsong@ustc.edu.cn](mailto:wgsong@ustc.edu.cn), [junz@ustc.edu.cn](mailto:junz@ustc.edu.cn)

Received: 15 August 2021 / Last revision received: 4 November 2021 / Accepted: 11 November 2021  
DOI: [10.17815/CD.2021.125](https://doi.org/10.17815/CD.2021.125)

**Abstract** Current studies about moving obstacles mainly focus on uncommon evacuation scenarios, while there lacks researches on common egress scenarios, such as evacuation from an exit. This study aims to prove that pedestrian flow through exit can be improved by the presence of a moving obstacle and investigate the effect of a moving obstacle on regulating pedestrian flow. Unidirectional pedestrian flow simulations based on social force model are conducted to study the influence of a moving obstacle, a mobile robot, on the pedestrian flow through an exit. The robot reciprocates parallel to the wall of the exit with a constant speed  $0.5m/s$ . The gap between the robot and the exit is set as  $1.0m$ . The pedestrians need to obey the rule of avoiding collision with the robot. By comparing the distributions of individual evacuation time with and without a moving obstacle, it is proven that the average evacuation time can be reduced by a moving obstacle obviously. The moving obstacle can lead to the inhomogeneous distribution of the crowd near the exit by observing the density profiles. Furthermore, the crowd near the exit is classified into four groups according to the movement directions (left or right) and the positions (the left or right part relative to the center of the exit) of the robot. It reveals that the moving obstacle impedes the evacuation for a small proportion of the pedestrians, but promotes the evacuation for the large proportion of the pedestrians by the analysis on the fundamental diagrams of the four groups.

**Keywords** Moving obstacles · unidirectional pedestrian flow · exit · social force model · density profile · fundamental diagram

## 1 Introduction

People are jammed at crowded places such as metro stations, stadia and shopping malls, which may cause potential risks of crowd accidents if the people cannot evacuate timely. To alleviate the congestion and enhance pedestrian flow in densely populated environments, there are many researchers proposing ideas to solve the problems in recent years. For example, increasing the width of egress routes, suitably setting zigzag-shaped geometries or obstacles in front of an exit, changing exit choices for some pedestrians and opening temporary passageways [1–3]. With the development of robot technology and consideration of the controllability of robots, some studies introduce mobile robots to influence the collective motion of pedestrian crowd for promoting pedestrian traffic efficiency based on the principle of human–robot interaction [3–5].

The researchers put robots in many pedestrian evacuation facilities to study the effects of the robot regulation on pedestrians [2–6]. In a very simplified exit scenario where individuals can take one of two paths to exit a hallway, it is successful to balance the densities on the two paths by using robots to disturb pedestrians' choices on the paths based on genetic algorithms to optimize the robots' behaviors [2]. In a scenario where two pedestrian flows cross vertically, two mobile robots are set at the locations where the two pedestrian flows have not crossed yet, respectively. With the periodic motion of the two robots, the congestion level is reduced and the average velocity of pedestrians is increased on the merging area [6]. Afterwards that, in a corridor which is composed of several controlled entrances and one exit, the pedestrians are required to treat mobile robots as obstacles and try to avoid collisions with robots when passing by them. It achieves the goal of the pedestrian flow in every section under robots' regulation [3]. Furthermore, in an egress scenario that two merging pedestrian flows moving through a bottleneck exit, it proves that mobile robots can regulate pedestrian flows to have a desired collective motion and verifies that the motion style of robots is of vital importance for the regulation effect [4]. Besides, exit is a common geometry in most of pedestrian facilities, and current studies mainly focus on the methods of increasing exit width and locating obstacles in suitable positions near an exit [7, 8]. Until today, there still lacks the studies that a robot regulates pedestrian flow through an exit. Comparing to the current regulation pedestrian methods at an exit, a mobile robot can deal with more complex evacuation scenarios, for example, it can adjust its own motion to match pedestrian densities, which are in a dynamic state in a real system [4, 5, 9, 10].

In this study, we aim to verify that a mobile robot (a moving obstacle) can promote pedestrian flow through an exit and show that the movement characteristics of the crowd influenced by a moving obstacle can be changed. There are two main contributions in this work. First, it fills in research gaps that a moving obstacle regulates on pedestrian flow at an exit, and the results show that a moving obstacle can benefit for pedestrian evacuation. Second, most of the evacuation environments are in static state in current evacuation studies, and the fundamental diagrams ignore the change of evacuation environments in gen-

eral [11]. However, the evacuation environments in this study are ever-changing because of the movement of the moving obstacle. We propose that the crowd should be classified into different groups to investigate the movement patterns of the groups as the evacuation environments change. The fundamental diagrams of the groups should be studied respectively. The remainder of the paper is as following. In section 2, evacuation model and the parameters of pedestrians and a moving obstacle are briefly described. Section 3 introduces the data extraction and processing methods used for analyzing simulation results. Section 4 shows the main simulation results and comparison with the scenarios without an obstacle. The concluding remarks are made in section 5.

## 2 Evacuation model and settings

The social force model is proved that it can reproduce the collective behavior of pedestrians in previous studies, such as the phenomenon of “faster is slower” and the arch formation of crowd [12, 13]. The equation is described as follows:

$$m_i \frac{d\vec{v}_i}{dt} = m_i \frac{v_i^0(t) \vec{e}_i^0(t) - \vec{v}_i(t)}{\tau_i} + \sum_{j(j \neq i)} \vec{f}_{ij} + \sum_W \vec{f}_{iW} + \varepsilon_i(t) \quad (1)$$

Where the motion of pedestrians is motivated by two type forces and a random turbulence. The first term of Eq. 1 means that the pedestrian  $i$  tends to move in the direction  $\vec{e}_i^0$  pointing to their own destination with a comfortable velocity  $v_i^0$ , which is usually called self-driven force. The second and third term of Eq. 1 respectively means that the pedestrian  $i$  is influenced by the pedestrian  $j$  and the surrounding environment  $W$ , which represent interaction force. The fourth term of Eq. 1 is random turbulence force  $\varepsilon_i$  for avoiding two or more pedestrians taking the similar behavior at the same moment.

The simulation scenario is a single-exit room, whose area is  $15m \times 20m$ . Considering that pedestrians have enough reaction time to the movement of the moving obstacle, the pedestrians are arranged on the left part of the room away from the moving obstacle. The specific scene layout is shown in Fig. 1(a). The desired velocity is set as 1.4m/s because it is the average velocity in normal evacuation for young pedestrians [14]. The settings for pedestrians are listed in Tab. 1. The movement rule of the moving obstacle is that the moving obstacle only moves parallel to the wall of the exit and keeps the gap of 1.0m with a constant speed of 0.5m/s (see Fig. 1(b)).

The key settings for the moving obstacle is according to the studies carried out by Shiomi et al. [15]. In their human-robot interaction experiments, they found that the behaviors of the pedestrians face to face passing through the robot just like those in the only humans involved experiments. The moving obstacle is a mobile robot in fact. Consequently, the force of the moving obstacle on pedestrian  $i$  can be referred to the second term of Eq. 1, and parameters can be referred in Tab. 1.

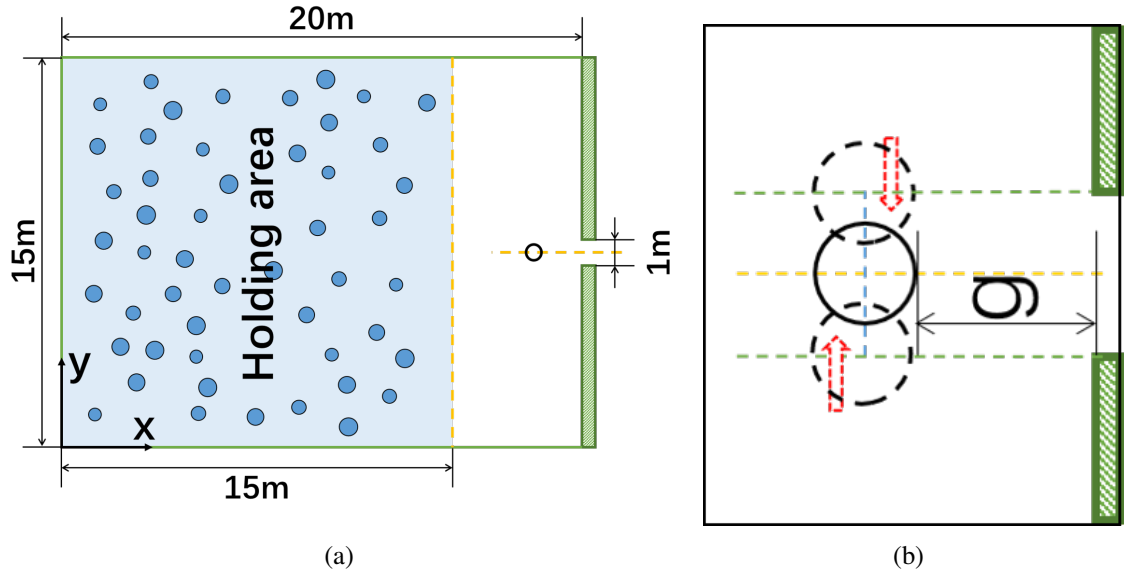


**Figure 1** (a) The layout of the simulation room. The blue disks represent pedestrians. The black circle is a moving obstacle. The pedestrians are uniformly distributed on the holding area, whose area is  $15m \times 15m$ , at the beginning of simulation. The origin of cartesian coordinate is set at lower left corner of the room (the remainder of the paper refers to this coordinate). (b) The sketch of the movement of the moving obstacle. The black circle in solid line is the beginning position of the moving obstacle. The two black circles in dashed line are the limit position for the moving obstacle. The red arrows represent the moving directions of the moving obstacle. The gap ( $g$ ) between the moving obstacle and the exit is  $1.0m$ .

Parameter	Value
Number of pedestrians	200
Desired velocity ( $m/s$ )	1.4
Radius of pedestrian ( $m$ )	0.25~0.35
Mass of pedestrian ( $kg$ )	60~80
$A_i$ ( $N$ )	$2 \times 10^3$
$B_i$ ( $m$ )	0.08
$\tau_i$ ( $s$ )	0.5
$k$ ( $kg \bullet s^{-2}$ )	$1.2 \times 10^5$
$\kappa$ ( $kg \bullet m^{-1} \bullet s^{-1}$ )	$2.4 \times 10^5$
$\varepsilon_i$ ( $N$ )	-10~10
Radius of moving obstacle ( $m$ )	0.3
Mass of moving obstacle ( $kg$ )	70
Time step length ( $s$ )	$1 \times 10^{-3}$

**Table 1** Settings of key parameters [12]

### 3 Data extraction and processing

By observation on the evacuation process, the stable stage is set as the time interval between the 10% and 80% pedestrians walking out the scenario [16]. The positions of the pedestrians are recorded every 0.1s. Each evacuation scenario is repeated five times.

In Sec. 4.1 of evacuation time, the spatial distribution of evacuation time is analyzed. That is a representation of the average time the pedestrians need to reach the exit from a location in the room. According to every pedestrian trajectory, the evacuation times at some locations belonging to the trajectories can be estimated. As for the evacuation times at the locations that may be not passed through by pedestrians are fitted based on a triangulation-based natural neighbor interpolation method [17].

In Sec. 4.2 of pedestrian density, Voronoi diagram method is applied to calculate pedestrian density [18]. The method is to build up Voronoi cell for the computation object (pedestrian) according to the surrounding environment. The density of the pedestrian on the corresponding Voronoi cell is the inverse of the area of the Voronoi cell.

In Sec. 4.3 of fundamental diagram, the calculation of pedestrian flowrate is based on the method proposed by Cao et al. [19]. It only considers the pedestrians who has contributions to the flowrate. The calculation rule is that the desired velocity can be projected to X-axis and Y-axis for setting those directions as positive. If the actual velocity component on X-axis is negative, then it is set to 0, or else it stays the same, which is also obeyed for the actual velocity component on Y-axis. The specific flow is the product of the pedestrian density and the processed actual velocity. As a comparison, the flow rate denoting the number of participants passing a line in a given time period is showed too [20].

## 4 Results

### 4.1 Evacuation time

To understand the effect of a moving obstacle on the single-exit room evacuation, the results of the pedestrian evacuation times are presented. The distribution of individual evacuation time reflects the evacuation time of single pedestrian. The relation between evacuation time and the number of pedestrians leaving the room reflects the stability of the evacuation process. From Fig. 2, it shows that the evacuation efficiency is improved by the moving obstacle because the maximum evacuation time and the average evacuation time are reduced. The proportion of pedestrians needing more than 70 seconds to evacuate decreases, even the proportion of pedestrians needing more than 100 seconds disappears on the condition of the moving obstacle. This illustrates that the moving obstacle can alleviate the congestion level comparing with the situation without a moving obstacle. Fig. 3 shows that the pedestrian flow is more stable with a moving obstacle, which is

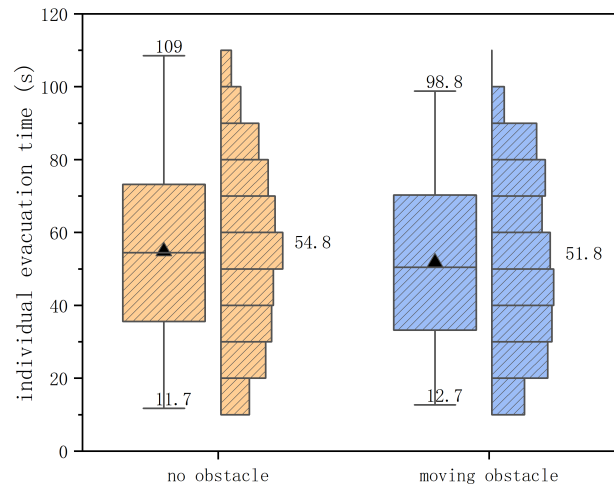


**Figure 2** The distributions of individual evacuation time at different evacuation scenarios. The minimum value, the maximum value and the average value are marked.

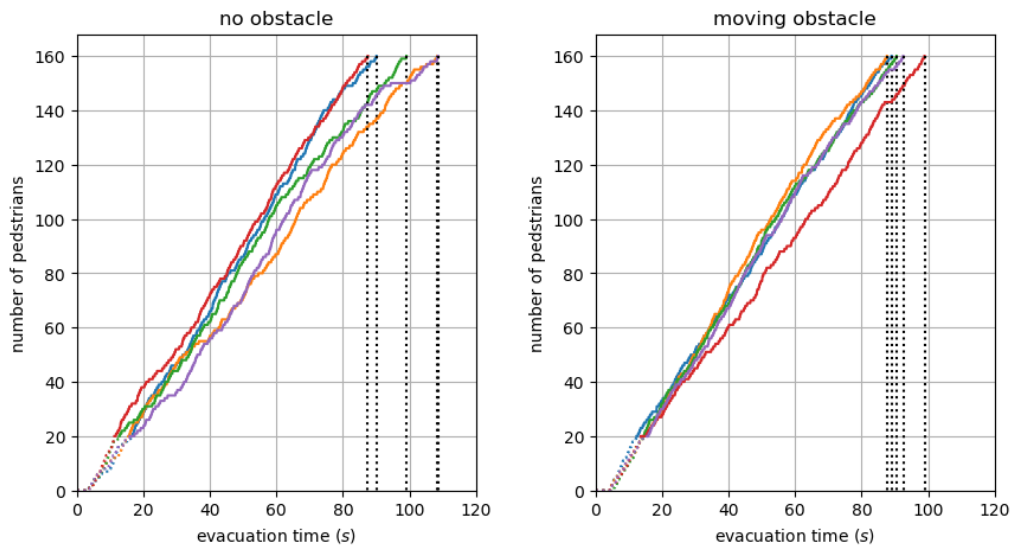


**Figure 3** The relation between evacuation time and the number of pedestrians leaving the room at different evacuation scenarios. The color dotted lines are out of consideration due to the evacuation phase not in stability. The solid lines in different colors means the results of different simulations.

reflected by the smooth slopes of the color lines and the concentrated range of the overall evacuation time for the five simulations.

By investigating the spatial distribution of evacuation time, it is possible to judge the evacuation difficulties at different locations in the room. Furthermore, in order to measure the evacuation resistance at different locations in the room, it needs to eliminate the influence of the distance between the location and the exit. Here is a normalization processing on the evacuation time, which is rescaled by  $r^2$  ( $r$ : the distance to the door). That can be understood by an ideal example. Assuming the flow rate and the density are constant near the exit, the number of the pedestrians around the exit is proportion to the area of  $\pi r^2$ , and the evacuation time is proportion to the number of the pedestrians around the exit. Hence, the evacuation time is proportion to the area of  $\pi r^2$ . This method has been proved reasonable in studies carried out by Zuriguel et al [17], whose evacuation scenario is also a single-exit room.

From Fig. 4(a), there is an interesting phenomenon. Under the evacuation condition with a moving obstacle, the evacuation time of the pedestrian flow from both sides that are close to the walls is apparently reduced comparing to the evacuation condition without obstacle. However, the pedestrian flow from the direction perpendicular to the door need more time to egress. It is easy to understand. As a moving obstacle impede the pedestrian flow directly passing through the exit, the pedestrians close to the walls can find a chance to escape quickly following the periodic movement of the moving obstacle. In Fig. 4(b) and Fig. 4(c), the evacuation resistance for the evacuation condition without obstacle mainly comes from both sides that are close to the walls but that on the direction perpendicular to the door is at a low level. However, the results of the evacuation condition with obstacle is completely reverse. From this observed phenomenon, we conjecture that the reason why the pedestrian flow is more fluent with a moving obstacle is that more pedestrians feel a lower evacuation resistance in the environment with a moving obstacle.

## 4.2 Pedestrian density

The pedestrian density is exhibited to figure out whether a moving obstacle can obviously influence the pedestrian density in the room. In this part, there are two formats to show the pedestrian density. One is the density profile of the whole room, another is the time series of the density around the exit. The measurement area is a semicircle of 2m in diameter, whose center is at the center of the exit, because it contains the pedestrians near the exit and the moving obstacle. And their trajectories show they are influenced perceptibly by the moving obstacle. As the moving obstacle is always in dynamic movement, we present the density profiles at some typical frames instead of averaging all frames. The pedestrian density calculated here is once at every 0.5s, so the 2 frames equals to 1s in Fig. 6.

In Fig. 6, it is apparent that the pedestrian density near the exit is reduced at most frames with a moving obstacle. We guess the reason is the presence of the moving obstacle makes

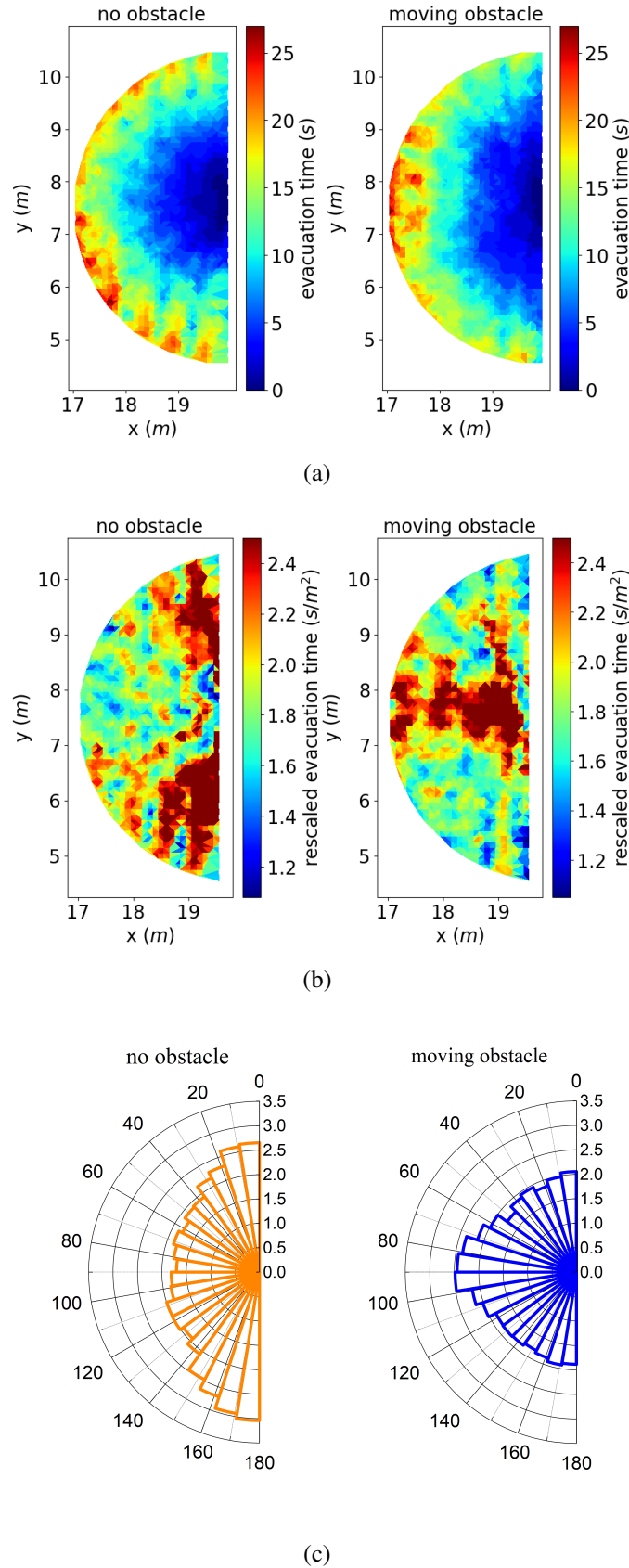


**Figure 4** Spatial dependence of the evacuation time at different scenarios. (a) The time taken to reach the door is displayed. (b) The evacuation time divided by  $r^2$  is shown. The door center is located at (20, 7.5). (c) The angle histogram of the rescaled evacuation times. Angles  $0^\circ$  and  $180^\circ$  correspond to pedestrians standing near the wall, and  $90^\circ$  to a direction perpendicular to the door. Radial units (gray semicircles) are  $s/m^2$ .

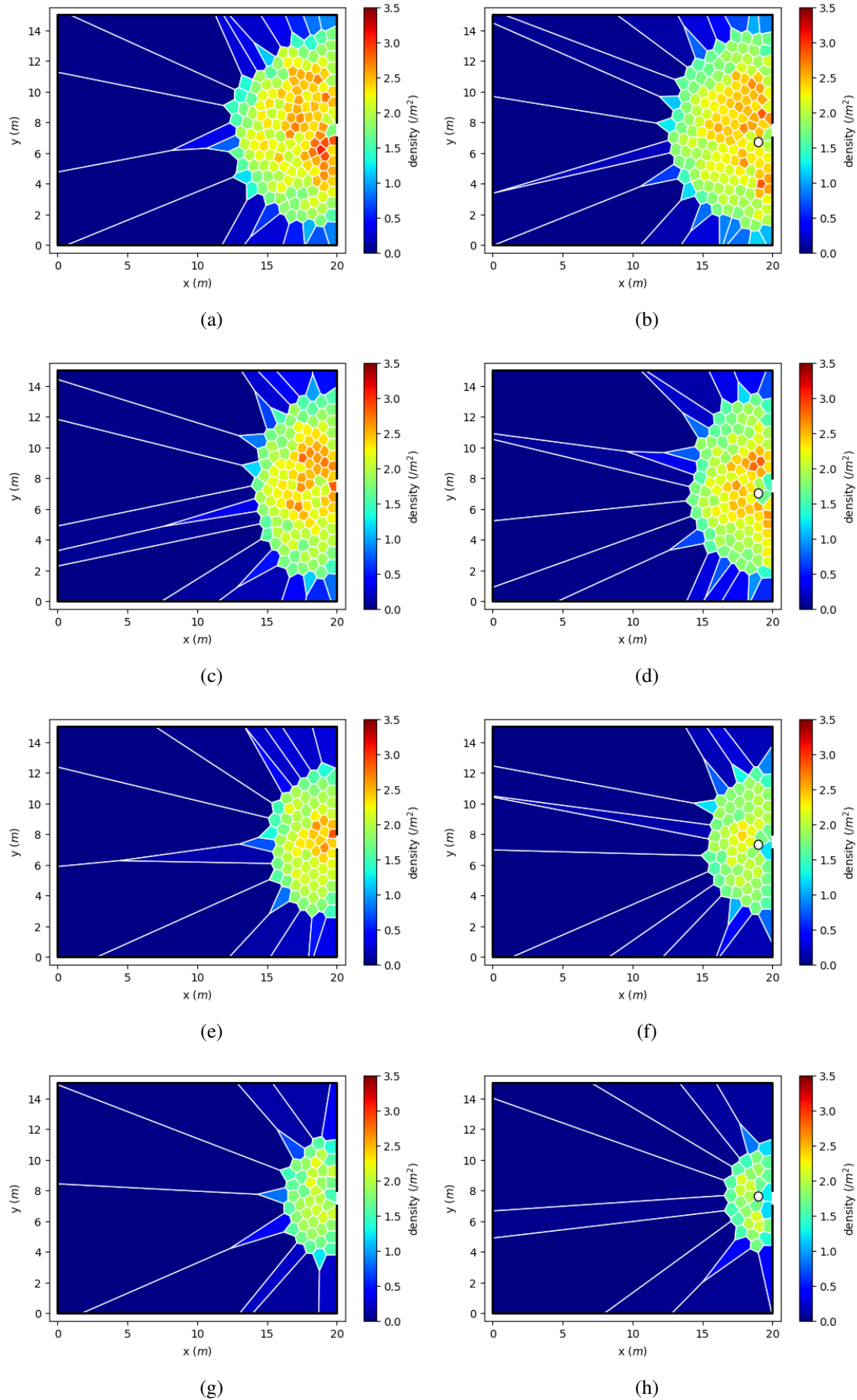


**Figure 5** The snapshots of the density profiles at different frames. The evacuation scenarios in first column including (a), (c), (e) and (g) are without obstacle and those in second column including (b), (d), (f) and (h) are with a moving obstacle. The time (frame) is at 0s in (a) and (b). The time (frame) is at 25s in (c) and (d). The time (frame) is at 50s in (e) and (f). The time (frame) is at 75s in (g) and (h).

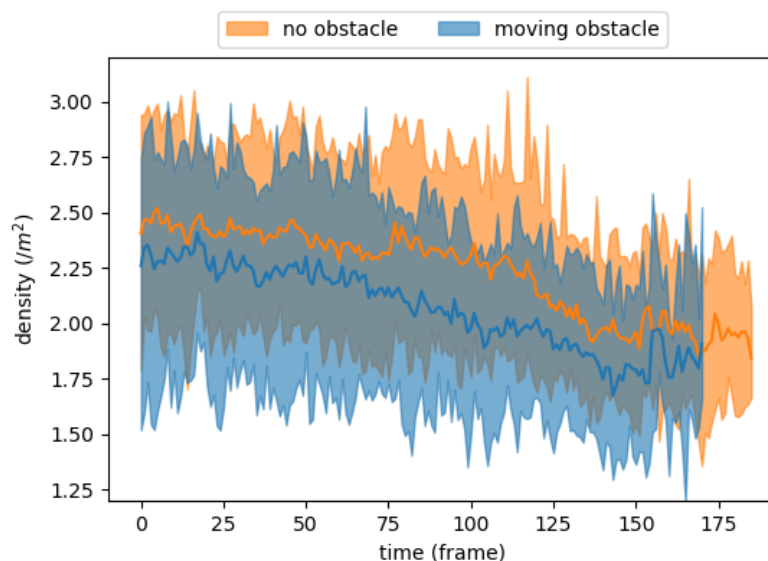


**Figure 6** The relation between the density of the pedestrians near the exit and time (frame) at different scenarios. The colored zone is the pedestrian density range and the color line is the average pedestrian density for five simulations.

more available space for pedestrians to escape, because the pedestrians around the moving obstacle will stay as far away from it as possible to have enough reaction time to avoid immediate contact with it. This is reflected in Fig. 5, the density around the moving obstacle is reduced comparing with the same position without obstacle. We also observe the phenomenon that the moving obstacle exacerbates the inhomogeneity of the density profile. In Fig. 5, the density around the exit is lower than that at other places. Besides, in Fig. 6, the pedestrian density range in the scenarios with the moving obstacle is wider than that in the scenarios without obstacle at most frames.

### 4.3 Fundamental diagram

Influenced by the periodic movement of the moving obstacle, the law of the motion exists difference for the pedestrians in different time and space. Hence, we roughly divide the observation area into four regions by regionA, regionB, regionC and regionD according to the position and velocity of the moving obstacle. Their different walking patterns can be clear by respectively observing their own fundamental diagrams.

The observation area is separated according to the movement period of the moving obstacle, and the whole movement period is separated into four parts, which is shown in Fig. 7. The first part is that the movement direction of the moving obstacle is on the positive direction of Y-axis and the position is on the positive direction of Y-axis relative to the central axis of the door. The second part is that the movement direction of the moving obstacle is on the negative direction of Y-axis and the position is on the positive direction of Y-axis relative to the central axis of the door. The regulations of the other two parts

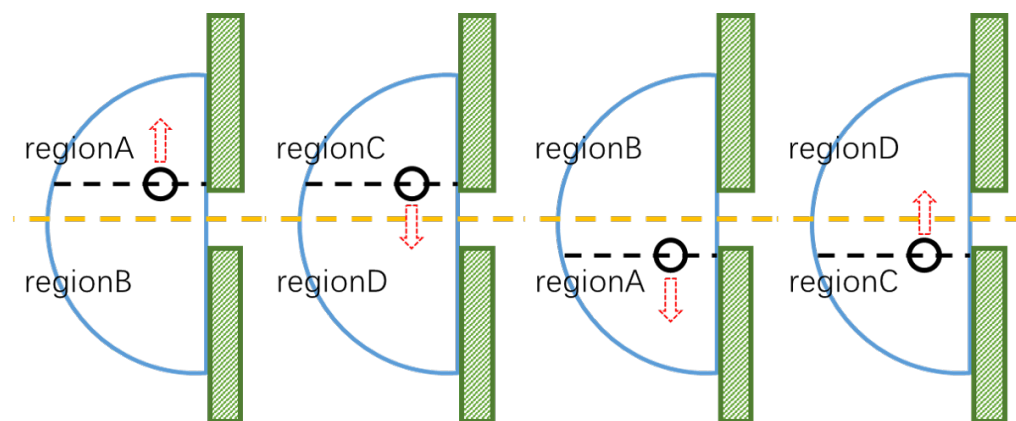


**Figure 7** The sketch of four regions on the observation area. The four subplots respectively represent a quarter of the movement period of the moving obstacle. The yellow dashed line is the central axis of the door. The black circle is the moving obstacle. The red arrow is the movement direction of the moving obstacle. The blue semicircle is an observation area. The dashed line passing through the center of the moving obstacle is used to separate the observation area.

are similar to these two parts, they are also according to the position and velocity of the moving obstacle. The area of regionA will be smaller and smaller with the movement of the moving obstacle and the pedestrians on it feel a “push” from the moving obstacle. The area of regionB will be bigger and bigger with the movement of the moving obstacle and the pedestrians on it will feel looser and looser. The scenarios on regionC are like those on regionB, but the path to exit is narrower. Hence, the pedestrians on it need a detour if they want to escape the room. The scenarios on regionD are like those on regionA, but the door is wider for pedestrians to escape. The measurement area is a semicircle of  $2m$  in diameter.

In Fig. 8, we obtain the information that the pedestrians on regionB and regionC can walk more fluently comparing to the pedestrians on regionA and regionD from observation on the distribution of specific flow. The distributions of density and specific flow for the pedestrians on regionD are like those for the pedestrians without obstacle, which means that the walking patterns of the pedestrians on regionD are close to those of the pedestrians without obstacle. As for the pedestrians on regionA, they are hard to walk out the room, even comparing to the evacuation scenario without obstacle. These phenomena fit with the original purpose of our region division, which is mentioned in the last paragraph where we analyze the feelings of pedestrians on different regions.

Furthermore, we piecewise average the scatters on Fig. 8 according to different densities to obtain Fig. 9(a). The data of Fig. 9(c) is obtained by averaging the scatters on Fig. 8. The densities on regionA, regionB, regionC and regionD are lower than those under the evacuation scenario without obstacle. However, the pedestrians on regionA almost cannot walk straight to the exit, even need to walk back to the room due to the “push” and obstruction of the moving obstacle, so the specific flow apparently is reduced. The spe-

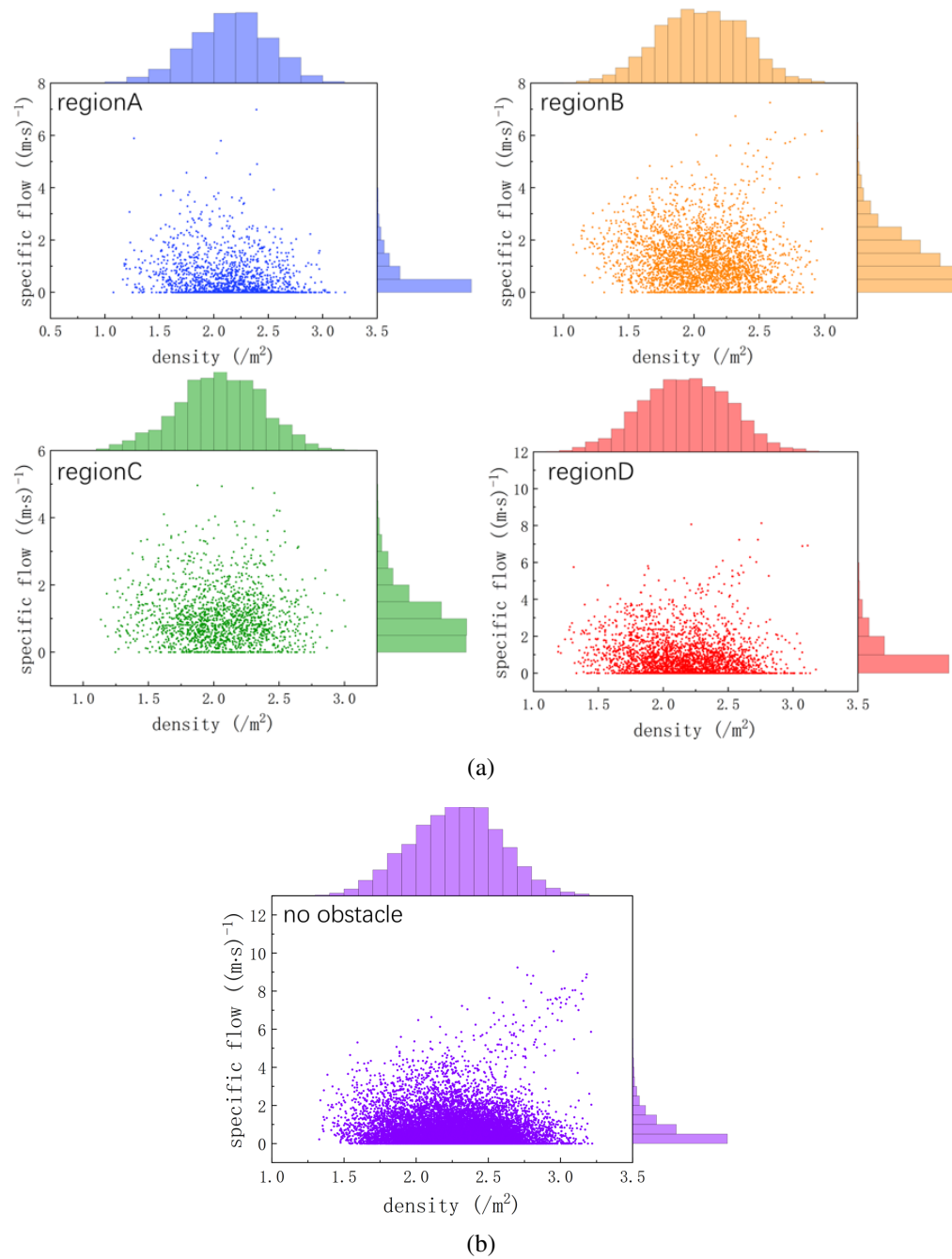


**Figure 8** Fundamental diagrams for the pedestrians on the four regions of regionA, regionB, regionC and regionD under the evacuation scenarios with the moving obstacle and that for the pedestrians under the evacuation scenarios without obstacle. The bars around the subplots are the density distribution of the scatters.

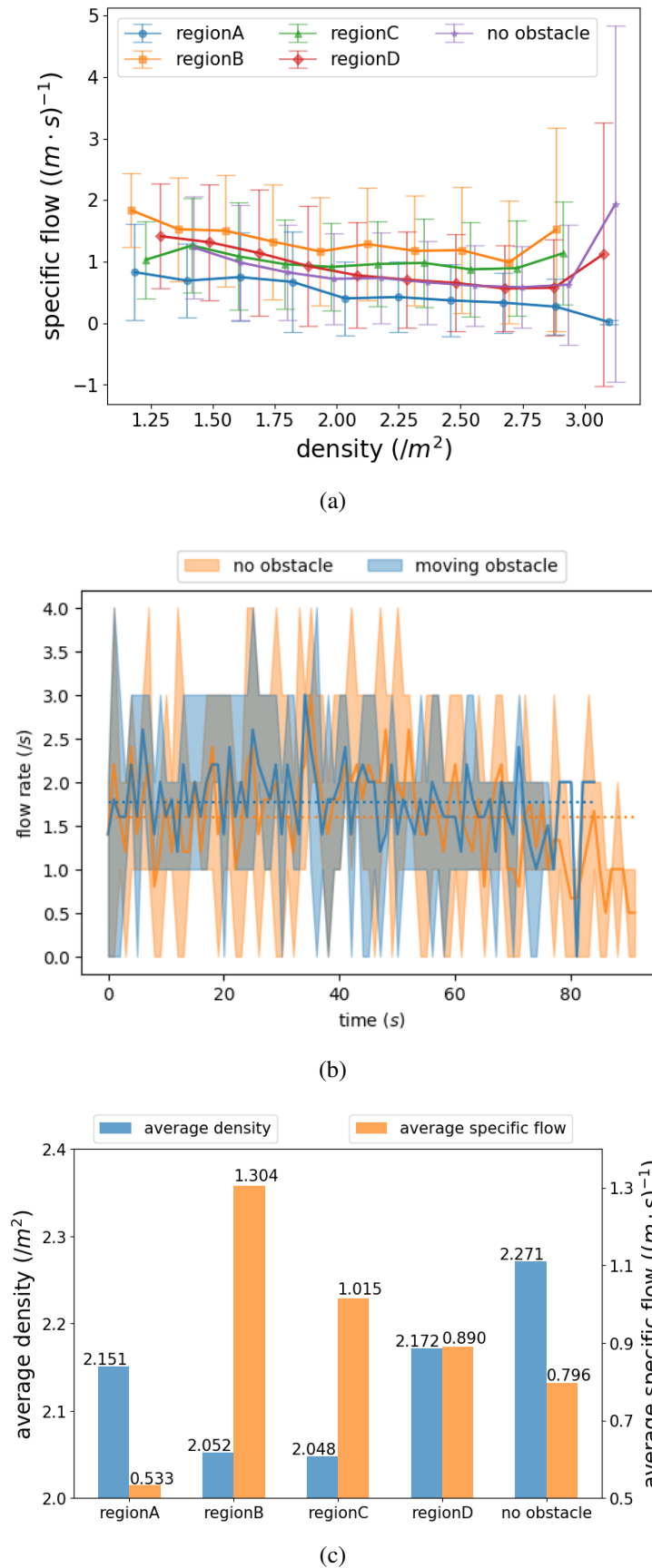


**Figure 9** (a) Average specific flow for the pedestrians on the four regions of regionA, regionB, regionC and regionD under the evacuation scenarios with the moving obstacle and that for the pedestrians under the evacuation scenarios without obstacle. Error bars have been calculated as the standard error with a confidence level of 95%. (b) The relation between flow rate and time. The dotted lines are the average of the flow rate. (c) The comparison of the average density and the average specific flow of the pedestrians with the moving obstacle on the four regions and the pedestrians without obstacle.

cific flow for regionB, regionC and regionD is improved at different levels comparing to the evacuation scenarios without obstacle. Besides, as the proportion of pedestrians on regionA and regionC is rather less than those on regionB and regionD (the number of pedestrians on the regions can be estimated by the integral of the area with respect to time), so the evacuation efficiency of the whole pedestrians can be improved. With the periodic movement of the moving obstacle, the pedestrians originally belonging to regionA also have chances to become the pedestrians belonging to regionB, regionC or regionD.

## 5 Conclusion

In this paper, we simulate the pedestrians evacuating from a single-exit room with a moving obstacle based on the social force model. The number of pedestrians in the room is 200, and the desired velocity is  $1.4m/s$ . The moving obstacle reciprocates parallel to the wall of the exit with a constant speed  $0.5m/s$ . Meanwhile the gap between the moving obstacle and the exit is set as 1.0m and the movement range of the moving obstacle equals to the width of the exit. The center of the movement range is across from the center of the exit. The pedestrians need to obey the rule of avoiding contact with the moving obstacle as much as possible and treat it as a “virtual pedestrian”.

It is obvious that the evacuation efficiency is improved with a moving obstacle. The pedestrian flow become fluent comparing to the scenarios without obstacle. The spatial distribution of evacuation time is influenced by the moving obstacle. The evacuation time for the pedestrians close to the walls of the exit is reduced but for the pedestrians, whose movement direction are perpendicular to the door, is increased compared to the results of the room without obstacle. The evacuation resistance, which equals to the ratio of evacuation time on a location in the room to the square of distance between the location and the exit, is introduced for showing more pedestrians at a lower evacuation resistance (less than  $2.0s/m^2$ ) with a moving obstacle. The moving obstacle exacerbates the inhomogeneity of the density profile near the exit. Meanwhile it makes the whole pedestrian density lower near the exit. We find differences in walking patterns of the pedestrians influenced by a moving obstacle. We divide the observation area into four regions according to the movement direction and the position of the moving obstacle. The fundamental diagrams of the four regions show that the specific flow for the three regions is improved at different levels but for another one region is reduced apparently. Besides, consideration of the different areas of the four regions, it can be concluded that there exists a period where less than half pedestrians in the room are impeded by the moving obstacle, but the period only exists about a half of the whole evacuation process. While the moving obstacle promotes the evacuation for more than three quarters of the pedestrians in the room.

**Acknowledgements** This work was supported by National Natural Science Foundation of China (52074252) and Anhui Key Research and Development Program (202004a07020052).

## References

- [1] D. Helbing, L. Buzna, A. Johansson, T. Werner, Self-Organized Pedestrian Crowd Dynamics: Experiments, Simulations, and Design Solutions, *Transportation Science*, 39 (2005) 1-24, [doi:10.1287/trsc.1040.0108](https://doi.org/10.1287/trsc.1040.0108)
- [2] B.D. Eldridge, A.A. Maciejewski, Using genetic algorithms to optimize social robot behavior for improved pedestrian flow, in: *2005 IEEE International Conference on Systems, Man and Cybernetics*, IEEE, 2005, pp. 524-529, [doi:10.1109/ICSMC.2005.1571199](https://doi.org/10.1109/ICSMC.2005.1571199)
- [3] L. Shan, L. Chang, S. Xu, C. Jiang, Y. Guo, Robot-assisted pedestrian flow control of a controlled pedestrian corridor, *International Journal of Advanced Robotic Systems*, 15 (2018) 1729881418814694, [doi:10.1177/1729881418814694](https://doi.org/10.1177/1729881418814694)
- [4] Z. Wan, C. Jiang, M. Fahad, Z. Ni, Y. Guo, H. He, Robot-assisted pedestrian regulation based on deep reinforcement learning, *IEEE transactions on cybernetics*, 50 (2018) 1669-1682, [doi:10.1109/TCYB.2018.2878977](https://doi.org/10.1109/TCYB.2018.2878977)
- [5] C. Jiang, Z. Ni, Y. Guo, H. He, Robot-assisted pedestrian regulation in an exit corridor, in: *2016 IEEE/RSJ International Conference on Intelligent Robots and Systems (IROS)*, IEEE, 2016, pp. 815-822, [doi:10.1109/IROS.2016.7759145](https://doi.org/10.1109/IROS.2016.7759145)
- [6] K. Yamamoto, M. Okada, Continuum Model of Crossing Pedestrian Flows and Swarm Control Based on Temporal/Spatial Frequency, *IEEE Int Conf Robot*, (2011), [doi:10.1109/ICRA.2011.5980444](https://doi.org/10.1109/ICRA.2011.5980444)
- [7] H. Li, J. Zhang, L. Yang, W. Song, K.K.R. Yuen, A comparative study on the bottleneck flow between preschool children and adults under different movement motivations, *Safety Sci*, 121 (2020) 30-41, [doi:10.1016/j.ssci.2019.09.002](https://doi.org/10.1016/j.ssci.2019.09.002)
- [8] T. Matsuoka, A. Tomoeda, M. Iwamoto, K. Suzuno, D. Ueyama, Effects of an Obstacle Position for Pedestrian Evacuation: SF Model Approach, in: *Springer International Publishing*, Cham, 2015, pp. 163-170, [doi:10.1007/978-3-319-10629-8\\_19](https://doi.org/10.1007/978-3-319-10629-8_19)
- [9] C. Jiang, Z. Ni, Y. Guo, H. He, Pedestrian Flow Optimization to Reduce the Risk of Crowd Disasters Through Human–Robot Interaction, *IEEE Transactions on Emerging Topics in Computational Intelligence*, 4 (2019) 298-311, [doi:10.1109/TETCI.2019.2930249](https://doi.org/10.1109/TETCI.2019.2930249)
- [10] C. Jiang, Z. Ni, Y. Guo, H. He, Learning human–robot interaction for robot-assisted pedestrian flow optimization, *IEEE Transactions on Systems, Man, and Cybernetics: Systems*, 49 (2017) 797-813, [doi:10.1109/TSMC.2017.2725300](https://doi.org/10.1109/TSMC.2017.2725300)
- [11] L.D. Vanumu, K.R. Rao, G. Tiwari, Fundamental diagrams of pedestrian flow characteristics: A review, *European transport research review*, 9 (2017) 1-13, [doi:10.1007/s12544-017-0264-6](https://doi.org/10.1007/s12544-017-0264-6)

- [12] D. Helbing, I. Farkas, T. Vicsek, Simulating dynamical features of escape panic, *Nature*, 407 (2000) 487-490, doi:10.1038/35035023
- [13] D. Helbing, P. Molnar, Social force model for pedestrian dynamics, *Phys Rev E Stat Phys Plasmas Fluids Relat Interdiscip Topics*, 51 (1995) 4282-4286, doi:10.1103/physreve.51.4282
- [14] X. Ren, J. Zhang, W. Song, S. Cao, The fundamental diagrams of elderly pedestrian flow in straight corridors under different densities, *Journal of Statistical Mechanics: Theory and Experiment*, 2019 (2019) 023403, doi:10.1088/1742-5468/aafa7b
- [15] M. Shiomi, F. Zanlungo, K. Hayashi, T. Kanda, Towards a Socially Acceptable Collision Avoidance for a Mobile Robot Navigating Among Pedestrians Using a Pedestrian Model, *Int J Soc Robot*, 6 (2014) 443-455, doi:10.1007/s12369-014-0238-y
- [16] Y. Zhao, T. Lu, L. Fu, P. Wu, M. Li, Experimental verification of escape efficiency enhancement by the presence of obstacles, *Safety Sci*, 122 (2020) 104517, doi:10.1016/j.ssci.2019.104517
- [17] I. Zuriguel, I. Echeverria, D. Maza, R.C. Hidalgo, C. Martin-Gomez, A. Garcimartin, Contact forces and dynamics of pedestrians evacuating a room: The column effect, *Safety Sci*, 121 (2019) 394-402, doi:10.1016/j.ssci.2019.09.014
- [18] B. Steffen, A. Seyfried, Methods for measuring pedestrian density, flow, speed and direction with minimal scatter, *Physica A: Statistical Mechanics and its Applications*, 389 (2010) 1902-1910, doi:10.1016/j.physa.2009.12.015
- [19] S. Cao, A. Seyfried, J. Zhang, S. Holl, W. Song, Fundamental diagrams for multidirectional pedestrian flows, *Journal of Statistical Mechanics Theory and Experiment*, 3 (2017) 033404, doi:10.1088/1742-5468/aa620d
- [20] A. Seyfried, O. Passon, B. Steffen, M. Boltes, T. Rupperecht, W. Klingsch, New insights into pedestrian flow through bottlenecks, *Transportation Science*, 43 (2009) 395-406, doi:10.1287/trsc.1090.0263